Solvation Dynamics of Coumarin 480 in TritonX-100 (TX-100) and Bile Salt Mixed Micelles†

ARTICLE *in* THE JOURNAL OF PHYSICAL CHEMISTRY A · JULY 2003

Impact Factor: 2.69 · DOI: 10.1021/jp0271458

3 AUTHORS, INCLUDING:

Partha Hazra
Indian Institute of Science Education and Re…
52 PUBLICATIONS **997** CITATIONS
SEE PROFILE

Nilmoni Sarkar
IIT Kharagpur
159 PUBLICATIONS **3,689** CITATIONS
SEE PROFILE

Solvation Dynamics of Coumarin 480 in TritonX-100 (TX-100) and Bile Salt Mixed Micelles†

Debdeep Chakrabarty, Partha Hazra, and Nilmoni Sarkar*

Department of Chemistry, Indian Institute of Technology, Kharagpur 721 302, WB, India

Received: October 7, 2002; In Final Form: May 7, 2003

The time-resolved Stokes' shift of the laser dye Coumarin 480 (C-480) has been investigated in the Stern layer of the pure Triton X-100 (TX-100), bile salt (Sodium Deoxycholate, NaDC) and the mixed micelles of bile salt (NaDC), and TX-100 at different compositions using picosecond time-resolved emission spectroscopy. The wavelength dependent decays at the blue end and growth at the red end of the spectrum are observed for the TX-100, NaDC micelles, and mixed micelles above critical micelles concentrations. The average solvation time in pure NaDC and TX-100 are 3.35 and 1.51 ns, respectively, but in the mixed micelles, it is 2.27−3.26 ns. The solvation dynamics of the water molecule in the Stern layer of the mixed micelles is retarded several times compared to that of pure water. The relatively slow solvation dynamics in the Stern layer of the NaDC micelles is due to the motion of the Na^+ ions and the water molecules confined in the micellar cavity. The interaction of the Na^+ ions with the headgroup of the micelle is also responsible for the slow dynamics. The slow dynamics in the mixed micelles compared to that of pure water is due to the motion of confined water in the micellar core, motion of the Na^+ ions, and interaction of the Na^+ ions with the headgroup of the micelles. In the mixed micelles, the solvation dynamics is relatively faster because of the removal of Na^+ ion from the Stern layer.

1. Introduction

The solvation dynamics of various polar molecules in microheterogeneous organized assemblies[1−4] and the protein surface[5] are of considerable interest in recent years. The self-organized microheterogeneous media are an interesting model for biological membranes, so there is a tremendous interest to study the solvation dynamics in restricted environments.[1−8] The self-organized assemblies have water molecules as an essential ingredient. Examples of such types of organized assemblies are abundant in nature, e.g., a water pool of reverse micelles, the surface of the micelles, and also the surface and interior of protein, etc.[9] Recently, the dynamics of water molecules in the restricted self-organized assemblies have been studied by various techniques, particularly dielectric relaxation[10] and solvation.[12−15] All of these experimental measurements emerge to an interesting result that the dynamics of water in these restricted environments is much slower compared to that of pure water and bimodal in nature. The bimodal response of confined water consists of a subpicosecond component and a very slow component of several hundreds to thousands of picoseconds.[2−8] However, the dynamics of pure water is studied extensively by solvation dynamics[1,12,13a,14,15d] and dielectric relaxation.[10,11] Pure water exhibits very fast solvation dynamics. Recently, Fleming et al.[1,12] also observed a very fast component of 30 fs in the solvation dynamics of Eosin dye in water using three photon echo peak shift (3PEPS) technique. The fast component in solvation dynamics of water in restricted environment is comparable to the bulk water, whereas the second slow component is completely absent in it. The slow second component appears to be unique in the complex system whose origin is yet to be clearly understood. Recently, Bagchi et al.[15b−c] proposed a dynamic exchange model for reverse micelles and proteins to explain the slow component. In this model,[15b−c] they assume a dynamic exchange between the "free" and the "bound" water molecules. The energetics of the exchange depends on the strength and number of the hydrogen bonds between bound water molecules and biomolecules. The increase in the strength of the hydrogen bond increases the relative population of bound water and also the slow component.

Several groups have observed the retardation of solvation dynamics in restricted environments.[1−9] Particularly, Bright et al.[6] studied the nanosecond solvation dynamics of reverse micelles using a biological fluorophore covalently attached to albumin and also using 1-anilinonaphthalene-8-sulfonic acid (1,8-ANS). The solvation dynamics is severely retarded compared to pure water studied by Bhattacharyya et al.[2,3] in reverse micelles using various probes. Recently, Levinger et al.[4] investigated the solvation dynamics in different reverse micelles using the femtosecond fluorescence upconversion technique and reported the retardation of the solvation dynamics in restricted geometries. Micelles are important restricted media where one can investigate solvation dynamics. These are generally spherical aggregates formed by the surfactant molecules in aqueous solution when the concentration of the surfactant exceeds a certain critical value known as the critical micellar concentration (CMC). Bhattacharyya et al.[8] studied the solvation dynamics in the Stern layer of the micelles, e.g., neutral (TX-100), cationic (cetyl trimethylammonium bromide, CTAB), and anionic (sodium dodecyl sulfate, SDS), using C-480 and 4-aminophthalimide (4-AP) as a probe. The existence of the probe in the Stern layer of the micelles is confirmed from steady state spectroscopic results. The average solvation times for TX-100, CTAB, and SDS are respectively 1450, 470, and 180 ps using C-480 and

† Dedicated to Professor Mihir Chowdhury on the occasion of his 65th birthday.

* To whom correspondence should be addressed. E-mail: nilmoni@chem.iitkgp.ernet.in. Fax: (91)-3222-255303.

10.1021/jp0271458 CCC: $25.00
Published on Web 07/12/2003

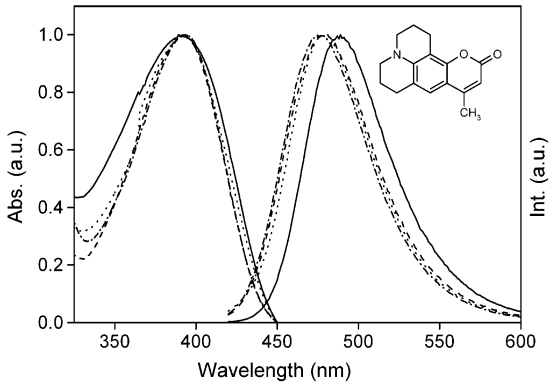

Figure 1. Steady-state absorption and emission spectra of C-480 in water and in pure and mixed micelles of TX-100 and NaDC. Solid lines for water, dashed lines for pure TX-100, dotted lines for pure NaDC, and dash−dot lines for 1:1 TX-100:NaDC mixed micelle. The molecular structure of C-480 is depicted in the inset.

SCHEME 1: Structure of Bile Salt

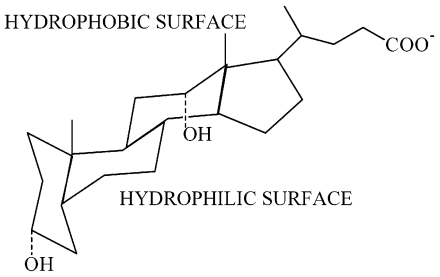

720, 270, and 80 ps using 4-AP.[8] Thus, the slow component of solvation dynamics in micelles is several times slower compared to the bulk water. In the present work, our major interest is to probe the solvation dynamics of Coumarin 480 (C-480, Figure 1) in the Stern layer of the mixed micellar aggregates of bile salt and TX-100.

Mixed micellar aggregates composed of a binary surfactant are of considerable interest from the viewpoint of fundamental, technological, pharmaceutical, and biological considerations.[17−20] Recently, considerable effort has been made to study the mixed aggregates of bile salts and synthetic detergents. Bile salts are biologically very important and play vital role in a number of physiological processes such as lipid, lecithin, and cholesterol solubilization and regulation of cholesterol.[21] In combination with ordinary detergents, bile salts are used in biochemicals and pharmaceutical properties as solubilizers for medicine. Bile salts are naturally occurring amphiphilic compounds which are synthesized in the liver and stored in the gallblader.[21b] In an ordinary surfactant, the alkyl chain coiled into a spherical micelle with a "dry" hydrocarbon core and the periphery of the micelles contain a water-filled spherical shell. This spherical shell is coiled into the Stern layer for ionic micelles and the Palisade layer for neutral micelles. The bile salts are different from ordinary surfactants and do not possess the polar headgroup or nonpolar aliphatic tail. The bile salt (NaDC) (Scheme 1) consists of a hydrophobic steroid ring and a hydrophilic moiety comprised of hydroxyl groups, a carboxylate anion, and a sodium cation. The steroid moiety in the bile salt is not planar. It consists of a hydrophobic moiety on its convex surface, but the hydroxyl groups are located on the concave side. This arrangement gives bile salt molecules planar polarity, which is crucial for spontaneous aggregation in aqueous solutions. Micellization of the bile salts and their interaction with the biological membrane play an important role in billiary secretion and cholesterol solubilization.[16,21] In a slightly alkaline medium,

SCHEME 2: Structure of Mixed Micelle

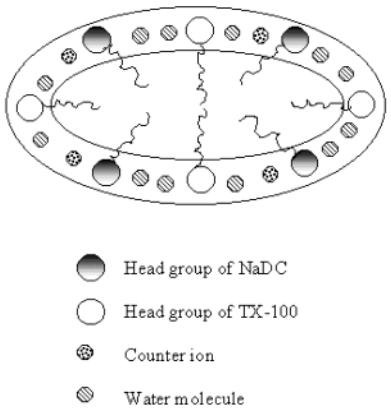

NaDC exhibits two CMCs at ∼10 and ∼60 mM which are referred to as primary and secondary micellar concentrations, respectively. The most popular model to explain the aggregation of the bile salt is Small's primary/secondary aggregation model.[21b] According to the model, the primary aggregations are formed by a small number of monomers (2−10) and can incorporate hydrophobic molecules within their core. With the increase in bile salt concentration, the primary aggregates associated to form large structure (secondary aggregates), in which the primary units are held together by hydrogen bonds between the hydroxyl and side chain group of the bile salts. From the recent small angel neutron scattering (SANS) studies,[22,23] the structure of the secondary aggregates resembles an elongated rod with a center hydrophilic core filled with water and ions. In the case of NaDC, the length of the rod is about 32 Å and the radius is ∼8 Å. The polarity of the core of the bile salt aggregates was estimated by Gouin et al.[24] Recently, Bohne et al.[25] investigated the triplet state quenching in bile salt aggregates.

Haque et al.[19] investigated in detail the mixed micellar properties of bile salt (sodium deoxycholate) and also an important synthetic detergent Triton X-100. The structure of the well-known micelles formed by the TX-100 (neutral), CTAB (cationic), and SDS (anionic) were established from small angle neutron scattering (SANS) measurements.[16] Each micellar aggregate contains 100−150 surfactant molecules. The radius is 50 Å for TX-100 micelle. The core of the micelles is essentially "dry" and contains the hydrocarbon chains only. At the periphery of the micelles, there is a "wet" shell of thickness 6−9 Å comprising the polar headgroup, the counterion, and a considerable amount of water. This shell is known as the Stern layer. It is polar but less polar compared to bulk water. The SANS data is not available for NaDC-TX-100 micellar aggregates but the available data of the thickness of the palisade layer for TX-100 micelle is 20 Å, and the dimension of the Stern layer for NaDC micelles is 8 Å.[16,22−23] The aggregation number of NaDC (10) micelles is less than that of pure TX-100 micelle (139), whereas the aggregation number of mixed micelles is of intermediate values (36−109). In the NaDC-TX-100 mixed micellar system, the Stern layer consists of the headgroups of both the surfactants and the counterion Na^+. A more realistic picture of mixed micelle can be drawn using the individual micellar structure (Scheme 2). Clint[26] proposed a phase separation model to describe the phenomena of mixed micelle formation. According to this model, ideal mixing of the surfactants in the micellar phase is assumed which permits calculations of the CMCs of the mixed entities in terms of the overall composition of the combined components and the CMC of the individual surfactant.

The ideal mixing theory has been quite successful in explaining the properties of surfactants having similar structures but can hardly account for the characteristics of mixed systems of dissimilar structure. When a nonionic surfactant (e.g., TX-100) is inserted into a micelle composed of ionic (e.g., NaDC) surfactants, the nonionic hydrophilic group separates charged ionic hydrophilic groups from each other, reducing the electrical repulsion in the Stern layer of the micelle.[17−18,27] In other words, the charge density at the micellar surface is retarded, which reduces the absolute value of electrical potential.[17,18] A more quantitative approach toward mixed micelle formation was put forwarded by Rubingh[20c] on the basis of regular solution theory. Though this theory is quite useful to predict the CMC of the mixed micelles but the theory has certain thermodynamic limitations. Recently, Puvvada et al.[20a−b] have developed a molecular thermodynamic model for mixed surfactant systems. We have reported here how the solvation dynamics of C-480 is affected in the Stern layer of the mixed micelles. We have not observed any time dependent Stokes' shift in *n*-heptane for C-480. The bulk water solvation time is 310 fs[1] using C-480 and it is too fast to be detected by our setup. The results we would like to report here are the solvation dynamics of C-480 in the Stern layer of the mixed micelles of NaDC and TX-100 at different compositions particularly pure TX-100, pure NaDC micelles and also at 1:9 NaDC:TX-100, 1:1 NaDC:TX-100, 3:1 NaDC:TX-100, and 9:1 NaDC:TX-100. In a mixed micellar solution, the concentration of the NaDC micelles is kept above the CMC of the primary aggregates. To the best of our knowledge, this is the first report of the measurement of solvation dynamics in the mixed micelle.

2. Experimental Section

Coumarin 480 (Laser grade from Exciton) was used as received. NaDC, Sigma chemicals, was 99% pure. It was purified by the literature procedure.[19] TX-100 was obtained from Aldrich and used as received. The aqueous solution of the surfactants and the mixed micelles were prepared by the literature procedure.[19] The concentration of C-480 in all of the measurements is 5×10^{-5} M. We have used Shimadzu (model no. UV1601) for absorption and Spex Fluorolog-3 (model no. FL3-11) for fluorescence measurements. The fluorescence spectrum was corrected for spectral sensitivity of the instrument.

The experimental setup for the picosecond time correlated single photon counting (TCSPC) is described elsewhere.[28] Briefly, a mode locked Ti:sapphire laser (Spectra Physics, Tsunami) pumped by cw visible laser (Spectra Physics, Milenia) was used as light source. The fluorescence signal was detected in magic angle (54.7°) polarization using Hamamatsu MCP PMT (3809U). The excitation wavelength for all time-resolved studies was 413 nm. The typical system response at 413 nm excitation is about ∼50 ps. For rotational relaxation studies, we used a picosecond laser diode at 408 nm of IBH (U.K.). The other parts are similar as that of the earlier setup. The typical system response using this laser is ∼75 ps. For the anisotropy measurement, we used motorized polarizer in the emission side. For rotational relaxation studies, the emission intensity at perpendicular ($I_\perp$) and parallel ($I_\parallel$) polarizations was collected alternatively for 30 s. For a typical anisotropy decay, the difference between the peak counts at parallel and perpendicular polarization are kept to 1000. The *G* factor of the setup was measured using the same dye. The analysis of the anisotropy decays was done by IBH DAS6 decay analysis software. The temperature was kept at 298 ± 1 K for all measurements. The analysis of the solvation dynamics data was done by the procedure used by Maroncelli and Fleming[12b] and described in our earlier publication.[28] The concentrations of NaDC and TX-100 micelles were kept at ∼10 and ∼1.1 mM. Moreover, the concentrations of the NaDC and TX-100 mixed micelles at different compositions were also kept above 4 times of the individual CMC.

TABLE 1: Steady State Absorption and Emission Spectra of C-480 in Pure TX-100, Pure NaDC, and Different Composition of Mixed Micelles

composition	λ_{abs}(max)/nm	λ_{em}(max)/nm
pure TX-100	389	475
pure NaDC	389	478
TX-100:NaDC (9:1)	390	474
TX-100:NaDC (1:1)	390	474
TX-100:NaDC (1:3)	394	477
TX-100:NaDC (1:9)	394	477
water	389	490

3. Results and Discussion

3.1. Steady-State Absorption and Emission Spectra. The absorption spectra of C-480 at the three different compositions of the mixed micelles above CMC (pure TX-100, 1:1 TX-100:NaDC, and pure NaDC) are shown in the Figure 1. It has to be pointed out that there is almost little change in the absorption spectrum as we move from pure water to the mixed micelle. However, on addition of surfactant to the water solution of the C-480, the emission spectrum remains more or less unaffected up to CMC. Above the CMC, the intensity of the emission spectra almost unchanged. However, there is a significant blue shift of the emission spectra of C-480 as we move from pure water to the mixed micelle. The maximum shift of emission spectra observed at 474 nm in case of 1:1 NaDC:TX-100 mixed micelle. The emission peak of C-480 in pure water is at 490 nm.[29] The peak positions at different compositions of the mixed micelles including pure water, TX-100, and NaDC micelles are listed in the Table 1. The blue shift in the emission spectra indicates that the probe molecule C-480 is transformed from the polar aqueous phase to the relatively nonpolar surface of the micelles. The peak position of C-480 in nonpolar media like *n*-heptane is around 410 nm. In the pure NaDC, TX-100 micelles, and also in the mixed micelles, the intensity of the emission spectra is very less around 410 nm. It indicates that very few probe molecules are residing in the hydrocarbon core of the micelle. The peak position is around 474 nm in the mixed micelle, which is very close to the emission peak of C-480 in pure ethanol.[29] It indicates that the polarity of the micellar surface should be close to that of ethanol. However, in a heterogeneous surface like micelle, the diffusional motion of the probe cannot be ignored. Consequently, the probe will sense an average polarity. It is better to state that the polarity of the micellar surface is less than that of water. To obtain a better insight into the location of the probe in the mixed micelles, steady-state fluorescence emission anisotropy (*r*) was determined using the following relation:

$$r = \frac{(I_{VV} - GI_{VH})}{(I_{VV} + 2GI_{VH})} \quad (1)$$

where *G* is the correction factor for detection sensitivity to the polarization direction of the emission and I_{VV} and I_{VH} represent the vertically and horizontally polarized emission intensity obtained on excitation with a vertically polarized light. The fluorescence anisotropy (*r*) of the dye C-480 in pure water and at different mixed micelle concentration is shown in the Table

TABLE 2: Decay Characteristics of $C(t)$ of Coumarin 480 (C-480) in Pure and Mixed Micelles of TX-100 and NaDC

composition	$\Delta\nu$ (cm^{-1})[a]	a_1	τ_1 (ns)	a_2	τ_2 (ns)	$\langle\tau\rangle$[b] (ns)
pure NaDC	420.41	0.503	0.73	0.492	6.06	3.35
TX-100:NaDC (9:1)	504.95	0.705	0.92	0.289	5.60	2.27
TX-100:NaDC (1:1)	505.82	0.699	0.87	0.294	6.14	2.41
TX-100:NaDC (1:3)	402.29	0.690	1.12	0.303	8.05	3.21
TX-100:NaDC (1:9)	481.28	0.615	0.86	0.377	7.24	3.26

[a] $\Delta\nu = \nu_0 - \nu_\infty$. [b] $\langle\tau\rangle = a_1\tau_1 + a_2\tau_2$.

TABLE 3: Calculated Time-Zero Fluorescence Maxima $\nu_{cal}(0)$, Observed Time-Zero Fluorescence Maxima $\nu(0)$, Time-Infinity Fluorescence Maxima $\nu(\infty)$, and Missing Components of Coumarin 480 (C-480) in Pure and Mixed Micelles

compositions	$\nu_{cal}(0)$[a] (cm^{-1})	$\nu(0)$ (cm^{-1})	$\nu(\infty)$ (cm^{-1})	missing component[b]
pure NaDC	22571.43	21070.781	20650.365	0.78
TX-100:NaDC(9:1)	22572.89	21325.929	20820.980	0.73
TX-100:NaDC(1:1)	22494.22	21275.427	20769.607	0.71
TX-100:NaDC(1:3)	22418.39	21118.144	20715.855	0.76
TX-100:NaDC(1:9)	22353.29	21131.643	20688.320	0.73

[a] Estimated from eq 3. [b] Calculated as $[\nu_{cal}(0) - \nu(0)]/[\nu_{cal}(0) - \nu(\infty)]$.

TABLE 4: Steady State Anisotropy (r), Initial Anisotropy (r_0), and Rotational Relaxation Time (τ_r) of C-480 in Pure Water, in Pure Micelles, and in Mixed Micelles

composition	r	r_0	a_{1r}	τ_{1r} (ns)	a_{2r}	τ_{2r} (ns)
pure NaDC	0.018	0.40	0.19	0.150	0.21	0.900
1:9 TX-100:NaDC	0.036	0.40	0.26	0.446	0.14	2.51
1:3 TX-100:NaDC	0.043	0.35	0.18	0.310	0.17	2.22
1:1 TX-100:NaDC	0.049	0.35	0.19	0.283	0.16	2.24
9:1 TX-100:NaDC	0.045	0.36	0.21	0.464	0.15	2.58
pure TX-100	0.024	0.37	0.18	0.090	0.19	1.43
pure water	0.002	0.40	0.40	0.125		

4. It is revealed from Table 4 that the fluorescence anisotropy value in pure water is much less and close to zero. On the contary, a high value of anisotropy is obtained in different mixed micelles. It indicates that the probe C-480 is transformed to the micellar surface from bulk water.

3.2. Sovation Dynamics. *3.2.1. Solvation Dynamics in Pure NaDC.* The few dye molecules in the hydrocarbon core of the micelles do not exhibit a time dependent Stokes' shift, and the dynamics in the bulk water[2-3,13-14] is too fast to be detected by our setup. However, at a ~10 mM concentration of NaDC (which is higher than the primary CMC of the NaDC), we have observed wavelength dependence decay at the blue end and red end of the emission spectrum. At 430 nm, the decay is clearly biexponential having two components of 1.56 (70%) and 4.49 ns (30%). However, at 550 nm, the decay consists of a clear growth of 810 ps and a decay of 6.4 ns. The existence of growth at the red end of the emission spectrum indicates that the probe (C-480) is undergoing solvation. To extract the time constant of the solvation in the Stern layer of the NaDC micelle, we have constructed the decay of solvent correlation function ($C(t)$) which is defined as

$$C(t) = \frac{\nu(t) - \nu(\infty)}{\nu(0) - \nu(\infty)} \quad (2)$$

where $\nu(0)$, $\nu(t)$, and $\nu(\infty)$ are the peak frequencies at time zero, t, and infinity, respectively. The peak emission frequency is estimated from the time-resolved emission spectra (TRES). The TRES in the NaDC micelle has been constructed by the method

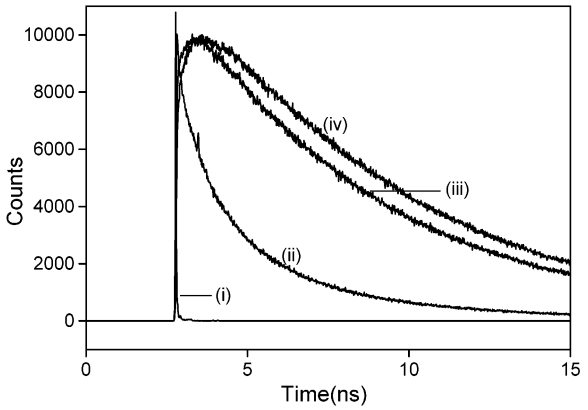

Figure 2. Fluorescence decays of C-480 in 1:9 TX-100:NaDC mixed micelle at (i) instrument response function (IRF), (ii) 430 nm, (iii) 470 nm, and (iv) 580 nm.

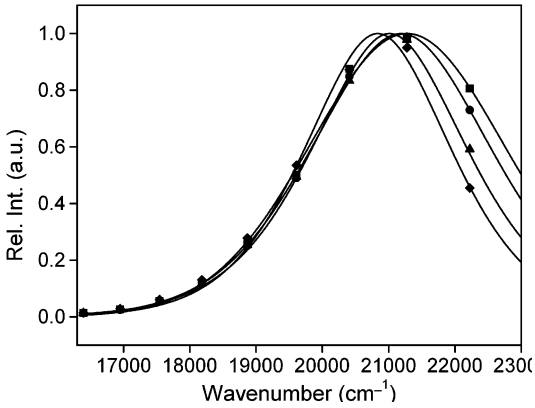

Figure 3. Time-resolved emission spectra of C-480 in 1:1 TX-100: NaDC mixed micelles at (i) 0 (■), (ii) 200 (●), (iii) 1000 (▲), and (iv) 5000 (◆) ps.

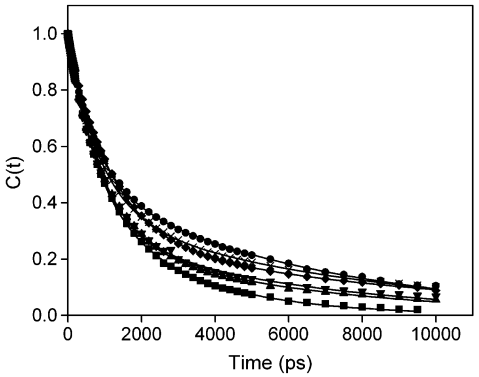

Figure 4. Decay of the solvent correlation function (C(t)) of C-480 in pure and mixed micelles of TX-100 and NaDC. (■) for pure TX-100, (●) for pure NaDC, (▲) for 9:1 TX-100:NaDC, (▼) for 1:1 TX-100: NaDC, (◆) for 1:3 TX-100:NaDC, and (×) for 1:9 TX-100:NaDC mixed micelle.

of Maroncelli and Fleming.[12b] The solvent correlation function ($C(t)$) of NaDC micelle is shown in Figure 4. After analyzing $C(t)$ with a biexponential fit, we have obtained solvation time of 730 ps (51%) and 6.06 ns (49%). The average solvation time is 3.35 ns in NaDC micelle.

3.2.2. Solvation Dynamics in Mixed Micelles. We have observed a distinct growth in the decay at the red end side of the emission spectra in all mixed micelles. The decay at the red end of the spectrum is significantly different from the blue end of the spectrum for all mixed micelles. Representative decays at different wavelengths of the 1:9 TX-100:NaDC mixed

micelle are shown in Figure 2. For example, the decay at 580 nm of 9:1 TX-100:NaDC micelle can be fitted with a biexponential function having a growth component of 1.07 ns and a decay component of 6.26 ns. However, the decay at 430 nm is single exponential with time constant of 2.06 ns. The wavelength dependent decay indicates time dependent Stokes' shift in the emission spectra. With an increase in time, the probe molecule is gradually solvated and it reduces the energy of the guest dipole. Consequently, the guest dipole will emit at the red end of the emission spectrum and exhibits a growth. A representative TRES at 1:1 TX-100:NaDC is shown in Figure 3. The variation of the solvent correlation function ($C(t)$) with respect to time (t) at different compositions of mixed micelles are shown in the Figure 4. The decay characteristics of $C(t)$ are summarized in Table 2. It is revealed from Table 2 that the average solvation time in pure NaDC micelle is 3.35 ns. On addition of TX-100 to NaDC, the average solvation time gradually decreases, and the solvation time at 1:1 NaDC:TX-100 is 2.41 ns, and at pure TX-100, the solvation time is 1.51 ns. The estimated value of solvation time in TX-100 micelle is very close to the reported value of 1.45 ns.[8a]

The most interesting observation of this experiment is slowing down of solvation dynamics (1.51−3.35 ns) in the Stern layer of the mixed micelle compared to the solvation dynamics of C-480 in pure water (310 fs).[1b] The solvation dynamics in mixed micelles is relatively slower compared to the solvation dynamics of C-480 in γ-cyclodextrin (γ-CD)[1b] as the solvation time in γ-CD is 480 ps. However, it is much faster compared to the relaxation of water molecules in the reverse micelles (1.2−8 ns)[2−4,6,28] and lipids (9 ns).[31] We have observed solvation time of 3.35 ns in the NaDC micelle. In case of bile salt aggregates (NaDC micelles), a major portion of water molecules remain bound to the hydroxyl group of the bile salt via hydrogen bonds and to the carboxylate sodium ions by electrostatic force. The motion of the water molecules in the bile salt cavity is restricted through these interactions, and we have observed a very slow dynamics. The stability of the mixed micelle formed by addition of TX-100 to the ionic NaDC micelle is explained from the thermodynamic standpoint. The nonionic surfactant reduces the electrical repulsion between the two charged ionic surfactants by staying between them.[26,27] The polar headgroup of the surfactants, counterions, and water molecules may be responsible for solvation in mixed micelles. The polar headgroups in the surfactant molecules are residing at the one end of the long alkyl chain, and the mobility of the headgroups will be much smaller because the chain dynamics is quite slow.[30] For instance, the dynamics in the polymer occurs in a ∼100 ns time scale. Thus, the solvation dynamics observed in the mixed micelles and pure TX-100 and NaDC micelles (1.51−3.35 ns) are contributed by the water molecules and the counterions present in the Stern layer. The TX-100 molecule consists of several oxygen atoms, and the water molecules can bind to these oxygen atoms. It may be a possible reason for the slow dynamics in mixed micelles. Nandi et al.[15b] earlier used a model to explain the slow dielectric relaxation in aqueous solution of protein and attributed the slow dynamics to the rate of exchange between "bound" and "free" water molecules. For instance, the slow dynamics in the molten salt is contributed by the translational motion of Na^+ ions.[32] The role of ions in the slow dynamics is further confirmed by Chapman et al.[33] The average solvation time in the mixed micelle is faster compared to pure NaDC. The most probable explanation is the removal of Na^+ ions from the Stern layer of the micelle with the subsequent increase of concentration of the neutral surfactant TX-100. In mixed micellar solution, the mutual diffusion of the surfactant may contribute to the solvation processes. However, we have not observed maximum solvation time at 1:1 composition of surfactant. This fact ruled out the mutual diffusion of the surfactant molecules.

It will be interesting to carry out a computer simulation study of the mixed micellar solution. Recently, some computer simulation studies have been carried out for the water molecules bound to micellar surface,[7] to the liquid−liquid interface,[35a] and in the water pool of microemulsions.[35b−c] These simulation results reveal slow dynamics in the solvation at the interface compared to the individual pure solvent. Recently, Balasubramanian et al.[7] executed a detailed molecular dynamics simulation study in cesium pentadecafluorooctanoate (CsPFO) in water and showed that the observed slow dynamics in the micellar surface is contributed by the interaction of the cesium ion with the polar headgroup and the orientational motion of the water molecules plays a secondary role.

In our present experimental setup using the TCSPC technique (time resolution ∼50 ps), we are missing a substantial amount of the fast component (less than 20 ps) in the solvation dynamics. In our case, we have excited the sample at 413 nm, which is very close to the absorption maximum (∼390 nm) of C-480 in the mixed micelles. We can apply the method applied by Maroncelli et al.[34] to calculate the missing component in the solvation dynamics. The time zero frequency can be estimated using the following relation from absorption and fluorescence spectra:

$$\nu_{p,md}(t=0) \approx \nu_{p,md}(abs) - [\nu_{np,md}(abs) - \nu_{np,md}(fl)] \quad (3)$$

where the subscripts 'p' and 'np' refer to the polar and the nonpolar spectrum, respectively, and the frequencies are not the values at maximum but correspond to the midpoint frequencies, ν_{md}, in the solvent. The observed time zero frequency, the time infinity frequency, and the percentage of missing component $[(\nu_{cal}(0) - \nu(0)]/[\nu_{cal}(0) - \nu(\infty)]$ are also listed in Table 3. On addition of NaDC to the TX-100 micelles, the mixed micelle is formed, and the missing component is gradually decreasing with the increase of the NaDC concentrations. This result seems to be reasonable because the solvation time in pure TX-100 is relatively faster. So, the possibility of the missing component will be more at higher TX-100 concentration. The percentage of the missing component is gradually decreasing in the mixed micelles. Recently, Fleming et al.[1] pointed out that the contribution of the slow relaxation is expected to be between 5 and 20%. Because the absorption spectra of C-480 in nonpolar solvent is not structureless, the reliability of the missing component is questionable according to Fee and Maroncelli.[34]

3.2.3. Time-Resolved Fluorescence Anisotropy Measurements. The rotational relaxation time is usually of the order of nanosecond time scale in the case of micelles. In case of mixed micelles, we have observed a solvation time of a nanosecond time scale. So, there is a possibility that the rotational motion of the probe may contribute to the solvation time.

To investigate the location of the probe in the mixed micellar solutions and also to find out the contribution of rotational relaxation in the solvation, we have measured time-resolved fluorescence anisotropy of C-480 in mixed micelles and pure NaDC and TX-100 micelles. The anisotropy decay ($r(t)$) is given by

$$r(t) = \frac{I_{||}(t) - GI_{\perp}(t)}{I_{||}(t) + 2GI_{\perp}(t)} \quad (4)$$

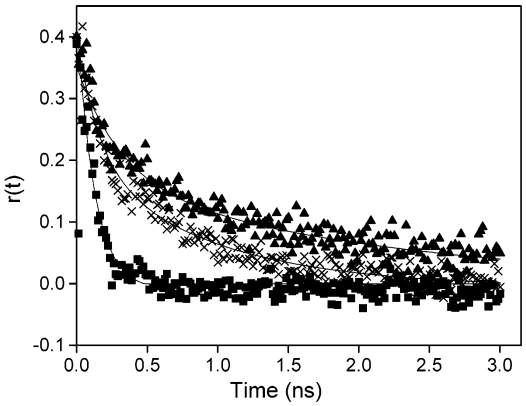

Figure 5. Decays of fluorescence anisotropy of Coumarin 480 in (a) pure water (■), (b) pure NaDC (×) micelle, and (c) 3:1 NaDC: TX-100 (▲) mixed micelle.

where $I_{||}(t)$ and $I_{\perp}(t)$ are fluorescence decays polarized parallel and perpendicular to the polarization of the excitation light, respectively. The fluorescence anisotropy decays of C-480 in pure water, pure NaDC, and 3:1 NaDC:TX-100 are shown in the Figure 5. The fluorescence anisotropy decays are fitted with a biexponential function in all mixed micelles and micelles. The results are shown in the Table 4. Various models such as the wobbling-in-a-cone and the two step model have been used to explain the biexponential rotational relaxation in micelles.[36] The anisotropy decay of C-480 in pure water is fitted with a single-exponential function and the anisotropy decay time in pure water is 125 ps. It indicates that the rotational relaxation is much slower within the mixed micelles compared to water. It is revealed from the Table 4 that the rotational relaxation time has two components; the first one in the picosecond time scale and the another in the nanosecond time scale in different mixed micellar composition and also in the pure NaDC and TX-100 micelles. Comparing the solvation time with the rotational relaxation time, it is revealed that there is a significant contribution of the rotational relaxation of the probe in the solvation. Bagchi et al. earlier reported that the self-rotation of the probe can contribute to solvation in unrestricted situation.[37] It is revealed from the Table 4 that the rotational relaxation time is much smaller than solvation time. Recently, McCarroll et al.[38] studied the time-resolved fluorescence anisotropy in mixed surfactant solution of TX-114 and sodium dodecyl sulfate (SDS), and the observed values of the rotational relaxation time are very much close to ours. The relatively high value of the rotational relaxation time of several nanoseconds in mixed micelles compared to pure (125 ps) water strongly suggests that the probe C-480 is most probably residing at the micellar surface. Fayer et al. observe a similar type of behavior in chromophore dynamics in micelles.[39]

4. Conclusions

In this work, we have observed that the C-480 molecule exhibited a time dependent Stokes' shift in the Stern layer of the micelle. The location of the probe in the Stern layer is confirmed by steady state and time resolved emission spectroscopy. The water molecules in the Stern layer of the pure NaDC, the TX-100, and the corresponding mixed micelles, cause the solvation. The interaction of the headgroup with the counterions is also a possible cause for solvation. In pure NaDC and TX-100, the solvation times are 3.35 and 1.51 ns, respectively. In the TX-100-NaDC mixed micelles, the solvation time is relatively slower compared to pure NaDC. The relatively slower value of solvation time in NaDC is presumably due to the presence of Na^+ ions and its interaction with the headgroups. The solvation dynamics is relatively faster in the mixed micelles compared to pure NaDC because of the removal of Na^+ ions from the mixed micelles. Moreover, the dynamics observed in the Stern layer of the mixed micelles using C-480 is several times slower compared to the ultrafast solvation dynamics of the probe in pure water.[1] The time constant of solvation dynamics in mixed micelles indicates that the water molecules in the Stern layer are retarded in comparison to the pure water but relatively faster compared to the water molecules in the reverse micelles[2−4,6,28] or lipids.[31]

Acknowledgment. The research work was supported by generous grant by SERC, Department of science and Technology (DST) and Council of Scientific and Industrial Research (CSIR), Government of India. Some of the picosecond time resolved measurements were carried out in the National Centre for Ultrafast Processes (NCUFP) in Chennai, India. The authors are indebted to Prof. P. Natarajan, the director, and Prof. P. Ramamurthy of this national center for their cooperation. The authors also acknowledge Ms. K. Indira Priyadarshini for her assistance in time resolved experiments. D.C. and P.H. are thankful to CSIR for research fellowships. N.S. acknowledges Prof. K. Bhattacharyya for his inspiration and encouragement throughout this work.

References and Notes

(1) (a) Lang, M. J.; Jordanides, X. J.; Song, X.; Fleming, G. R. *J. Chem. Phys.* **1999**, *110*, 5884. (b) Vajda, S.; Jimenez, R.; Rosenthal, S. J.; Fidler, V.; Fleming, G. R.; Castner, E. W., Jr. *J. Chem. Soc., Faraday Trans.* **1995**, *91*, 867.

(2) Nandi, N.; Bhattacharyya, K.; Bagchi, B. *Chem. Rev.* **2000**, *100*, 2013.

(3) Bhattacharyya, K.; Bagchi, B. *J. Phys. Chem. A* **2000**, *104*, 10603.

(4) Levinger, N. E. *Curr. Opin. Colloid Interface Sci.* **2000**, *5*, 118.

(5) Pal, S. K.; Peon, J.; Zewail, A. H. *Proc. Natl. Acad. Sci. U.S.A.* **2002**, *99*, 1763.

(6) (a) Lundgren, J. S.; Heitz, M. P.; Bright, F. V. *Anal. Chem.* **1995**, *67*, 3775. (b) Zhang, J.; Bright, F. V. *J. Phys. Chem.* **1991**, *95*, 7900.

(7) Balasubramanian, S.; Bagchi, B. *J. Phys. Chem. B* **2001**, *105*, 12529.

(8) (a) Sarkar, N.; Datta, A.; Das, S.; Bhattacharyya, K. *J. Phys. Chem.* **1996**, *100*, 15483. (b) Datta, A.; Mandal, D.; Pal, S. K.; Bhattacharyya, K. *J. Mol. Liq.* **1998**, *77*, 121.

(9) Robinson, G. W.; Chu, S. B.; Singh, S.; Evans, M. W. *Water in Biology, Chemistry and Physics*; World Scientific: Singapore, 1996.

(10) (a) Mashimo, S.; Kuwabara, S.; Yagihara, S.; Higasi, K. *J. Phys. Chem.* **1987**, *91*, 6337. (b) Fukuzaki, M.; Miura, N.; Shinyashiki, N.; Kurita, D.; Shioya, S.; Haida, M.; Mashimo, S. *J. Phys. Chem.* **1995**, *99*, 431.

(11) (a) Kaatze, U. *Chem. Phys. Lett.* **1993**, 2031. (b) Telgmann, T.; Kaatze, U. *J. Phys. Chem. A* **2000**, *104*, 1085. (c) Mittleman, D. M.; Nuss, M. C.; Colvin, V. L. *Chem. Phys. Lett.* **1997**, *275*, 332.

(12) (a) Jimenez, R.; Fleming, G. R.; Kumar, P. V.; Maroncelli, M. *Nature* **1994**, *369*, 471. (b) Maroncelli, M.; Fleming, G. R. *J. Chem. Phys.* **1987**, *86*, 6221.

(13) (a) Maroncelli, M. *J. Mol. Liq.* **1993**, *57*, 1. (b) Horng, M. L.; Gardecki, J. A.; Papazyan, A.; Maroncelli, M. *J. Phys. Chem.* **1995**, *99*, 17311.

(14) (a) Jarzeba, W.; Barbara, P. F. *Adv. Photochem.* **1990**, *15*, 1. (b) Jarzeba, W.; Walker, G. C.; Johnson, A. E.; Kahlow, M. A.; Barbara, P. F. *J. Phys. Chem.* **1988**, *92*, 7039.

(15) (a) Chandra, A.; Bagchi, B. *Adv. Chem. Phys.* **1990**, *80*, 1. (b) Nandi, N.; Bagchi, B. *J. Phys. Chem. B* **1997**, *101*, 10954. (c) Nandi, N.; Bagchi, B. *J. Phys. Chem. A* **1998**, *102*, 8217. (d) Roy, S.; Bagchi, B. *J. Chem. Phys.* **1993**, *99*, 9938.

(16) (a) Berr, S. S.; Caponetti, E.; Johnson, J. S.; Jones, R. R. M., Jr. *J. Phys. Chem.* **1986**, *90*, 5766. (b) Berr, S. S.; Coleman, M. J.; Jones, R. R. M., Jr.; Johnson, J. S. *J. Phys. Chem.* **1986**, *90*, 6492.

(17) Scamehorn, J. F. In *Phenomena in Mixed Surfactant System*; Scamehorn, J. F., Ed.; ACS Symposium Series 311; American Chemical Society: Washington, DC, 1986.

(18) Khan, A.; Marques, E. F. *Curr. Opin. Colloid Interface Science* **2000**, *4*, 402.

(19) (a) Haque, M. E.; Das, A. R.; Rakshit, A. K.; Moulik, S. P. *Langmuir* **1996**, *12*, 4084. (b) Haque, M. E.; Das, A. R.; Moulik, S. P. *J. Phys. Chem.* **1995**, *99*, 14032.

(20) (a) Puvvada, S.; Blankschtein, D. *J. Phys. Chem*. **1992**, *96*, 5567. (b) Sarmoria, C.; Puvvada, S.; Blankschtein, D. *Langmuir* **1992**, *8*, 2690. (c) Rubingh, D. N. In *Solution Chemistry of Surfactants*; Mittal, K. L., Ed.; Plenum: New York, 1979; Vol. 1, p 337. (d) Hydration Processes in Biological and Macromolecular systems. *Faraday Discuss*. **1996**, *103*, 1−394.

(21) (a) Carey, M. C. In *The Liver: Biology and Pathobiology*; Arias, M., Pope, H., Schachter, D., Shafritz, D. A., Eds.; Raren Press: New York, 1982; Chapter 27, p 429. (b) Small, D. M. *The Bile Acid*; Plenum: New York, 1971; Vol. 1, p 302.

(22) Hjlem, R. P.; Schteingert, C. D.; Hofmann, A. F.; Thiagrajan, P. *J. Phys. Chem. B* **2000**, *104*, 197.

(23) Santhanlakshmi, J.; Shantha Lakshmi, G.; Aswal, V. K.; Goyal, P. S. *Proc. Indian Acad. Sci. Chem. Sci.* **2001**, *113*, 55 and refernces there in.

(24) Gouin, S.; Zhu, X. X. *Langmuir* **1998**, *14*, 4025.

(25) Ju, C.; Bohme, C. *J. Phys. Chem.* **1996**, *100*, 3847.

(26) Clint, J. H. *J. Chem. Soc., Faraday Trans*. *1* **1975**, *76*, 1327.

(27) (a) Funasaki, N.; Hada, S. *J. Phys. Chem.* **1979**, *83*, 2471. (b) Schick, M. J. *J. Am. Oil Chem. Soc.* **1966**, *43*, 681. (c) Birdi, K. S. *Proc. Int. Conf. Colloid Surf. Sci*. **1975**, *1*, 473.

(28) Hazra, P.; Sarkar, N. *Chem. Phys. Lett.* **2001**, *342*, 303.

(29) Jones, G., II.; Jackson, W. R.; Choi, C.; Bergmark, W. R. *J. Phys. Chem.* **1985**, *89*, 294.

(30) (a) Cassol, R.; Ge, M.-T.; Ferrarini, A.; Freed, J. H. *J. Phys. Chem B* **1997**, *101*, 8782. (b) Datta, R.; Choudhury, M.; Winnik, M. A. *Polymer* **1995**, *36*, 4445.

(31) Datta, A.; Pal, S. K.; Mandal, D.; Bhattacharyya, K. *J. Phys. Chem. B* **1998**, *102*, 6114.

(32) (a) Bart, E.; Huppert, D. *Chem. Phys. Lett*. **1992**, 195, 37. (b) Bart, E.; Meltsin, A.; Huppert, D. *J. Phys. Chem*. **1994**, *98*, 32.

(33) Chapman, C. F.; Maroncelli, M. *J. Phys. Chem*. **1991**, *95*, 9095.

(34) Fee, R. S.; Maroncelli, M. *Chem. Phys.* **1994**, *183*, 235.

(35) (a) Michael, D.; Benjamin, I. *J. Chem. Phys.* **2001**, *114*, 2817. (b) Faeder, J.; Ladanyi, B. M. *J. Phys. Chem. B* **2000**, *104*, 1033. (c) Senapathy, S.; Chandra, S. *J. Chem. Phys* **1999**, *111*, 207.

(36) (a) Balabai, N.; Linton, B.; Napper, A.; Priyadarshy, S.; Sukharevsky, A. P.; Waldeck, D. H. *J. Phys. Chem. B* **1998**, *102*, 9617. (b) Krishna, M. M. G.; Periasamy, N.; *Chem. Phys. Lett.* **1998**, *298*, 359.

(37) Bagchi, B.; Oxtoby, D. W.; Fleming, G. R. *Chem. Phys.* **1984**, *86*, 257.

(38) McCarrol, M. E.; Joly, A. G.; Wang, Z.; Frieddrich, D. M.; Wandruszka, R. V. *J. Colloid Interface Sci.* **1999**, *218*, 260.

(39) (a) Weidemair, K.; Tavernier, H. L.; Chu, K. T.; Fayer, M. D. *Chem. Phys. Lett.* **1997**, *276*, 309. (b) Weidemair, K.; Tavernier, H. L.; Fayer, M. D. *J. Phys. Chem. B* **1997**, *101*, 9352.